*Environ. Sci. Technol.* **1998**, *32,* 1176−1182

# Multifractal Analysis of Particle Size Distributions in Soil

HÉLÈNE GROUT,[†,‡]
ANA M. TARQUIS,[‡] AND
MARK R. WIESNER*,[§]

*Department of Environmental Science and Engineering, MS317, 6100 Main Street, Rice University, Houston, Texas 77005-1892, and Department of Applied Mathematics, E.T.S. Ingenieros Agrónomos, Polytechnic University of Madrid, Ciudad Universitaria sn, 28040 Madrid, Spain*

Power-law scaling of particle size distributions in air, water, and soil have been frequently reported and are sometimes interpreted in the context of a fractal dimension to yield estimates of the geometrical characteristics of particles and aggregates such as their density or porosity. However, the underlying process leading to a measure of particle size distribution suggests that, in general, particle size distributions in natural systems should not conform to a simple power law. Rather, *measures* on a fractal object such as a particle aggregate give rise to a very different type of scaling known as multifractal. In this paper, data on soil grain size distributions obtained from soil horizons composed predominantly of clay and silt are analyzed to illustrate the inappropriateness of a simple power law interpretation in this case and to demonstrate the theoretically anticipated multifractal behavior.

## Introduction

Fractal geometry has been applied to the description of numerous solid phases encountered in environmental systems including particle size distributions of clay aggregates in water (*1*), biological aggregates and marine snow (*2*, *3*), flocs produced in water and wastewater treatment (*4*, *5*), and aerosol agglomerates (*6*) to name a few. Fractal interpretations and earlier power-law behaviors of the distribution of mass of fragmented materials in soils produced by weathering processes have been reported over a period of nearly 30 years (*7*−*9*). Indeed, communications describing fractal representations of sediments and soils are abundant in the literature as evidenced by review articles by Thompson et al. (*10*) and, more recently, Tyler and Wheatcraft (*11*, *12*). A key objective in applying fractal geometry in previous studies has been to obtain a more fundamental descriptor of soils that can be related to the particle size distribution, the pore size distribution, and more macroscopic properties such as porosity, erodability, and, ultimately, soil water properties.

One of the most fundamental physical properties of soils and sediments is their texture (percentages of clay, silt, and sand). These quantities represent simple characteristics of the particle size distribution (PSD) and are widely used in soil classification as well as for estimation of numerous soil properties such as capillary pressure, permeability, porosity, water retention (*13*), thermal conductivity, and adsorption properties of chemicals (*14*). Perhaps because PSD and textural analysis are among the most common descriptors of field soils, measurement and quantification are often done simply using sieves, with results reported as summary statistics such as the mean grain diameter and the uniformity coefficient. However, in the past decade, considerable interest has developed in very detailed study of soil structure by a range of complementary methods such as mercury porosimetry and image analysis at different size scales or levels of organization (*15*−*17*). Investigators have turned to fractal geometry in search of more fundamental parameters to characterize soils (*8*, *11*). Bartoli et al. (*16*), using image analysis of silty and sandy soils concluded that the fractal approach appears to be a potentially useful tool for understanding the underlying processes in the creation or destruction of soil structure and texture.

Inherent in many of these studies dealing with both soils and the earlier cited works concerning suspended aggregates is the notion that the particle size distribution in these systems represents a distribution of mass from a real (as in the case of a soil) or conceptual object (as in the case of the population of aggregates in a suspension), which has a self-similar distribution of mass with respect to length scale. There is a large conceptual leap from applying fractal geometry to describe mass distribution within *an object* at different length scales to describing the distribution of *a measure* such as the mass- or number-based particle size distribution. The primary purpose of this communication is to suggest that, in general, particle size distributions in natural systems should not conform to simple power-law scaling. One implication of this suggestion is that attempts to calculate the "fractal dimension" of aggregates from the shape of the size distribution of those aggregates are likely to lead to incorrect conclusions regarding the characteristics of those aggregates such as their density or porosity. In theory, *measures* on a fractal object such as a particle aggregate give rise to a very different type of scaling known as multifractal, in which case a single power-law exponent (or fractal dimension) may not hold over the entire range of the measure. In this paper, we illustrate, using grain size distributions in soil, the in appropriateness of a simple power-law interpretation and demonstrate the theoretically anticipated multifractal behavior.

## Theory

**Fractals and Power Laws.** Fractal geometry is based on the idea of self-similarity, that is, the manner in which variations of an object are repeated at another scale (*18*, *19*). When an apparently irregular geometry manifests itself in a similar fashion that is independent of the scale at which an object is observed, a power law can be used to describe the measurable properties of the object (*20*). This scale invariance or self-similarity concept has become widely applied in several properties of natural soils, one of them being the particle size distribution (PSD).

If a fractal object in $M$-dimensional space is covered by $M$-dimensional "cubes" having a side length $\delta$, the number of such cubes, $N(\delta)$, needed to cover the object varies as $\delta^{-D}$ when $\delta \rightarrow 0$:

$$N(\delta) = C\delta^{-D} \tag{1}$$

* Corresponding author. Tel: (713) 285 5129. Fax: (713) 285 5203. E-mail: wiesner@rice.edu.

[†] Present address: Department de Geologia Dinamica, Geofisica i Pal., Facultat de Geologia, Campus de Pedralbes, 08071 Barcelona, Spain.

[‡] Polytechnic University of Madrid.

[§] Rice University.



S0013-936X(97)00434-3 CCC: $15.00 © 1998 American Chemical Society
Published on Web 03/21/1998

where $C$ is a proportionality constant and $D$ is the Haussdorf–Besicovitch dimension, commonly referred as the fractal dimension (*18*). Power laws of this type have been applied to describe the mass distribution of objects ranging from stars in galaxies to colloids in aggregates. In these examples, the fractal dimension (Haussdorf–Besicovitch dimension) is related to the physical scale or size of the geometric object under consideration (*21*).

Numerous attempts have also been made to fit power laws to particle size distributions in air or water as well as grain size distributions in soils. Tyler and Wheatcraft (*11*, *12*) used such a power law to describe the cumulative PSD based in number of soil particles ($N$) or mass of soil particles ($M$) as follows:

$$N(R \leq r) = C_1 R^{-D} \tag{2}$$

$$M(R \leq r) = C_2 R^{3-D} \tag{3}$$

where $N(R \leq r)$ is the number of particles of size $R$ or greater and $M(R \leq r)$ is the mass of particles of size $R$ or greater. $C_1$ and $C_2$ are proportionality constants, and $D$ is the fractal dimension of the soil.

Later work has shown that there are several problems in using a simple power law or fractal dimension as a descriptor for the distribution of mass at various length scales in soils. Different values of $D$ are obtained using $N(R \leq r)$ or $M(R \leq r)$, which perhaps draw into question the scale invariance of particle density (*22*, *23*). Also, Perfect et al. (*24*) have shown that a single value of $D$ may not be applicable across all size classes, perhaps leading one to concluded that different values of $D$ apply at different scales for the same soil.

**Multifractals.** The preceding discussion suggests that power-law behavior of particle size distributions is frequently not observed and therefore cannot be expected to hold as the general case. Moreover, the "fractal dimension" calculated from a power-law fit of PSD data and the fractal dimension(s) of objects making up that distribution are very different quantities. Methods for arriving at the fractal dimension of aggregates in a suspension from their PSD have been proposed (e.g., ref *2*). However, the conditions required to meet the assumptions imbedded in such analyses are highly constraining and there is no basis for determining whether these conditions will be satisfied in natural systems.

In contrast, theory suggests that particle size distributions should not be described by a single fractal dimension except under very restrictive conditions. Rather, the conditions leading to particle (or aggregate) size distributions in nature would lead us to anticipate that PSDs should display "multifractal" behavior. For example, a multiplicative generating process in which a measure varies over a nonuniform fractal gives rise to a multifractal distribution of that measure (*20*). Such might be the case if the PSD is viewed as a measure distributed over an object such as a soil or a suspension having a spatial distribution of mass, which is itself fractal. Alternatively, the PSD might be viewed as a measure which represents the ensemble of multiple interrelated processes such as degradation, weathering, precipitation, and aggregation. In either case, the measure (PSD) may display a self-similarity referred to as "multifractal" (*25*).

For example, in this work soil texture is studied in terms of the percentage of volume distributed in different particle sizes obtained from measurements with an electrical sensing zone (ESZ) type particle counter. If a constant density is assumed for all particles, volume measurements may be expressed as mass. Thus, one measure may be taken as the fraction of soil particle mass (or equivalently volume), $p_i$, in a size class "$i$". In this work, the support of this measure is the set of real numbers corresponding to particle diameters from 0.48 to 20 $\mu$m. This interval encompasses particles classified as clay or silt and includes to a very good approximation 100% of the soil material examined in this work. The lower bound of this support corresponds to the limit of detection of typical ESZ instruments. Thus, $p_i$ can be interpreted as the probability of finding soil particles of a certain mass within particle size interval "$i$" and it follows that $p((0.48,20]) = 1$ (or 100%). However $p$ may be spread over the interval (0.48,20] in such way that the concentration of mass varies widely.

With this definition of a probability measure, $p_i$, the idea of fractal dimension is extended by considering the various moments, $q$, of the measure normalized by their sum:

$$\mu_i(q,\delta) = \frac{p_i^q}{\sum_{i=1}^{n(\delta)} p_i^q} = \frac{p_i^q}{\mu(q,\delta)} \tag{4}$$

where $n(\delta)$ is the number of subintervals of size $\delta$ in largest interval (0.48,20], $\mu_i$ is the percentage of volume in the subinterval $i$, and $q$ is the weight or moment of the measure. The sum in the denominator of eq 4, $\mu(q, \delta)$, is dominated by the highest values of $p_i$ when $\delta \rightarrow 0$ if $q > 0$ and by the smallest values of $p_i$ if $q < 0$. In an analogous sense, averages of particle diameter are skewed to the high end of particle diameter when the average is based on particle volume, and the lower end when based on particle number. The similarlity of eq 4 to a partition function suggests an analogy with thermodynamics which is exploited in interpreting the resulting scaling functions.

A log–log plot of a selfsimilar measure, $\mu(q, \delta)$, vs $\delta$ at various values for $q$ will give:

$$\mu(q,\delta) \sim \delta^{-\tau(q)} \tag{5}$$

where $\tau(q)$ is called the $q$th mass exponent (*20*). If eqs 5 and 1 are compared, $\tau(q)$ is seen to play the role of a fractal dimension but it is not constant over all length scales, $\delta$. Instead, if $\tau(q)$ is plotted vs $q$, a multifractal measure will yield a convex function (*26*).

Results can be expressed in terms of the measure's multifractal spectrum, $f(\alpha)$, which is defined by a Legendre transformation as follows:

$$\alpha(q) = -\frac{d}{dq}\tau(q) \tag{6}$$

$$f[\alpha(q)] = q\alpha(q) + \tau(q) \tag{7}$$

where $\alpha$ is the Lipschitz–Hölder exponent or "crowding index" of the data, which characterizes the average strength of singularity in the measure $\mu$ (*27*). The quantity $f(\alpha)$ may be interpreted as the fractal dimension of the subset of the interval (0.48,20] that dominates the sum in eq 4 for different weights $q$ having the same Lipschitz–Hölder exponent ($\alpha$) (*26*).

The $f(\alpha)$ curve typically has a parabolic shape. A particularly meaningful parameter from the spectrum is the entropy dimension of the measure, defined for the case when $q = 1$, as

$$\alpha_1 = \alpha(1) = f[\alpha(1)] \tag{8}$$

The entropy dimension of the subset describes the uniformity of the measure, a value of 1 corresponding to a uniform spread (*26*).

## Materials and Methods

Despite the enormous importance of the PSD in soils, surprisingly few studies (e.g., ref *6*) have used electronic

**TABLE 1. Main Characteristics of the Different Horizons of the Soil Studied[a]**

| horizon | depth | description | OC (%) | pH (in $H_2O$) | mineralogical composition (%) | | | |
|---|---|---|---|---|---|---|---|---|
| | | | | | Sm | Q | F | C |
| 1 | ≈0−50 cm | very firm, dark gray clay | 0.511 | 8.20 | 79 | 21 | 0 | 0 |
| 2 | ≈50−80 cm | very firm, yellowish red clay | 0.395 | 8.73 | 76 | 19 | 2 | 3 |
| 3 | ≈90−120 cm | very firm, yellowish brown clay with light olive brown concretions | 0.0675 | 8.27 | 70 | 25 | 2 | 3 |

[a] OC = organic carbon; Sm = smectites; Q = quartz; F = feldspar; C = calcite.

**TABLE 2. Texture of the Studied Horizons Determined by Sieving and Coulter Counter**

| size classe | | horizon 1 | | horizon 2 | | horizon 3 | |
|---|---|---|---|---|---|---|---|
| | | sieves and sedimentation | coulter counter | sieves and sedimentation | coulter counter | sieves | coulter counter |
| <2 μm | % clay | 17 | 23.41 | 13.8 | 31.16 | 72 | 38.57 |
| 2−60 μm | % silt | 65 | 58.59 | 82.8 | 65.44 | | 33.43 |
| 60 μm−20 mm | % sand | 13.85 | | 2.74 | | 24.32 | |
| >20 mm | % gravel | 4.15 | | 0.59 | | 3.68 | |

particle counters to determine the particle size distribution in soils. In this work, an electronic sensing zone (ESZ) type particle counter (Coulter Multisizer Counter) was used to obtain enough data points in mass and number of soil particles coming from different horizons to allow a multifractal analysis.

**Soil.** Samples were obtained from three soil horizons (collected in September 1996) of the Lake Charles−urban complex association found in Houston. The pH of the soil was measured after immersing the samples in deionized water using an Orion Expandable Ion Analyzer EA 920 (*28*). The OC (organic carbon) analyses were determined using a carbonaceous analyzer (method 9060) by Inchcape Testing Services at Houston. The global mineralogical composition was determined by X-ray diffraction (Phillips 42202 diffractometer, Co anticathode). The conditions used for this analysis are 25 min from 3 to 78° $2\theta$ for the global characterization of powder disoriented and 15 min from 3 to 33° $2\theta$ for oriented preparations of clay minerals. Ethylene glycol treatment was made for smectite identification.

**Particle Size Distribution Analysis.** The bulk horizon samples were oven-dried (37 °C) and then sieved using a nest of ASTM sieves with mesh openings of 8 (2.36 mm), 10 (2 mm), 12 (1.68 mm), 14 (1.168), 16 (1.180), 18 (1 mm), 20 (0.85 mm), 25 (0.707 mm), 30 (0.6 mm), 35 (0.5 mm), 40 (0.425 mm), 45 (0.354 mm), 50 (0.3 mm), 60 (0.25 mm), 70 (0.212 mm), 80 (0.18 mm), 120 (0.125 mm), 140 (0.106 mm), 170 (0.09 mm), 200 (0.075 mm), and 230 (0.063 mm). For the finest sieves, the samples were washed through the sieves using tap water and then oven-dried. The 230 mesh opening, at approximately 63 μm, was used to separate the clay + silt fraction (defined as the fraction < 60 μm) from the sand + gravel fraction (fraction >60 μm). The clay fraction (<2 μm) for the horizons 1 and 2 was isolated from the silt fraction (2−60 μm) by sedimentation as estimated by Stoke's law (*29*). It was not possible to separate the clay and silt fractions in horizon 3 by sedimentation. The initial quantities of horizon samples and each retentate on the sieves were normalized in order to express each retentate in mass percentage.

The particle size distributions of the clay and silt fractions were obtained by suspending soil material in water and analyzing the suspensions with an electronic particle counter (Coulter Multisizer, Coulter Electronics Ltd., Luton, England). This instrument operates on the electrical sensing zone principle and allows for quantitative measurements of the volume and size of particles in suspension larger than approximately 0.48 μm. Accuracy of this method is limited to particles having diameters between 2 and 50% of the orifice diameter. For this reason, measurements using several orifices may be necessary to determine the size distribution of suspensions containing particles that differ considerably in size. Preliminary analyses showed that the silt and clay fractions of the samples contained almost no particles larger than 20 μm. Both 19 and 50 μm apertures were used for particle measurements in this work. Analyses were performed in a 2% NaCl electrolyte solution (by weight). Samples were dispersed mechanically 30 min and left wetted 1 day before analysis to allow the clay particles (smectite) to absorb water into their structure. Before each measurement, samples were sonicated 3 min to break up potential aggregates of particles. The analyses were replicated three times. The volumes given by the Coulter Counter were converted into mass assuming a value of 2.65 g/cm$^3$ for their density (*31*) to allow comparison of data from the electronic particle counter with data on particle mass passing through sieves. The results were expressed as weighted mass percentages of the clay and silt fractions determined after separation by sieving and sedimentation. Mass percentages were reconverted to number fractions using the following relationship:

$$N_i = \frac{6M_i}{2.65\pi d_i^{\,3}} \tag{9}$$

where $N_i$ is the number of particles, $M_i$ the mass, and $d_i$ is the diameter of particles (assumed to be spherical) in class "$i$". Thus, two different measures were considered in the multifractal analysis: one based on the mass and the other one based on the number of particles.

**Evaluation of Power Law Scaling.** Under the assumption of constant power law, scaling of the PSD's calculation of the "fractal dimension" of the PSD was carried out in two steps: first with the data obtained from the sieves and second with the data obtained from the analyses of the silt and clay fractions made using the electronic particle counter. The diameters of the particle sizes ($2r$) were used to fit a regression line between log $M(2r > 2R)$ and log($2R$), the slope of which is $S$, where:

$$M(2r > 2R) \sim (2R)^S \tag{10}$$

An estimate of the fractal dimension for the distribution of mass by size class comparable to those reported by previous

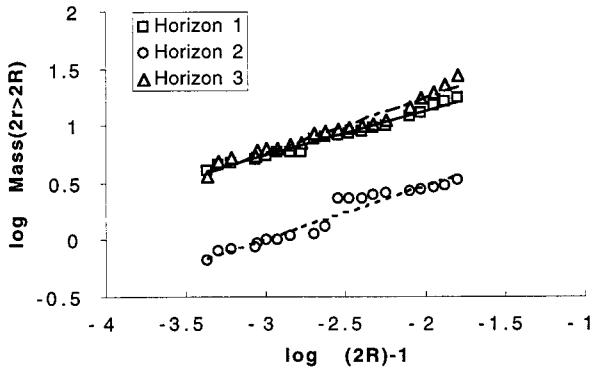


**FIGURE 1. log mass vs log(2*R*)$^{-1}$ for sand and gravel fractions for the three horizons. Lines are the calculated regression lines given in Table 3.**

**TABLE 3. Linear Regression between log(2*R*)$^{-1}$ and log[*M*(2*R*> 2*r*)]**

| horizon | number of points | $R^2$ | slope ± se | constant ± se | *D* (3-slope) |
|---|---|---|---|---|---|
| 1 | 20 | 0.98 | 0.388 ± 0.011 | 1.913 ± 0.026 | 2.612 |
| 2 | 20 | 0.93 | 0.467 ± 0.029 | 1.416 ± 0.064 | 2.533 |
| 3 | 20 | 0.96 | 0.473 ± 0.022 | 2.195 ± 0.048 | 2.527 |

investigators (*11*) is calculated from the slope, *S*, as

$$D = 3 - S \tag{11}$$

Subsequent analysis demonstrates that the mass distribution through the size classes is not adequately described by a single fractal dimension. Rather, a multifractal approach is shown to yield a more valid representation of the data.

**Calculation of Multifractal Spectrum.** The determination of the multifractal spectrum, $f(\alpha)$, was done for each horizon using 217, 152, and 175 points, respectively, for the horizons 1, 2, and 3. Because the mass percentage was predominantly in the clay fraction and silt fraction (with most of the particles ≤ 20 $\mu$m) in all the horizons, the study was done in the size range from 0.48 to 20 $\mu$m inclusive.

Several methods have been proposed to calculate $f(\alpha)$ such as the histogram method and the method of moments (*26*). For experimental data with a low dimension, as in the current case, a direct determination of the $f(\alpha)$ as suggested by Chhabra and Jensen (*32*) is preferable.

The following relationships were applied to calculate $f(q)$ and $\alpha(q)$ from the normalized measures [$\mu(0.48,20) = 1$] of mass and number:

$$f(q) = \lim_{\delta\to 0}\frac{\sum_{i=1}^{n(\delta)}\mu_i(q,\delta)\log[\mu_i(q,\delta)]}{\log\delta} \tag{12}$$

$$\alpha(q) = \lim_{\delta\to 0}\frac{\sum_{i=1}^{n(\delta)}\mu_i(q,\delta)\log[\mu_i(1,\delta)]}{\log\delta} \tag{13}$$

$f(\alpha)$ is then obtained by plotting $f(q)$ vs $\alpha(q)$ for each value of $q$. Equation 12 is essentially a restatement of the Boltzmann formula for statistical entropy when $q = 1$ at which value it is clear by comparison with eq 13 that $\alpha(1) = f(1)$. The "entropy dimension," $f(1)$, also referred to as the information dimension within the context of information theory, can be expressed as a function of a random variable's standard deviation.

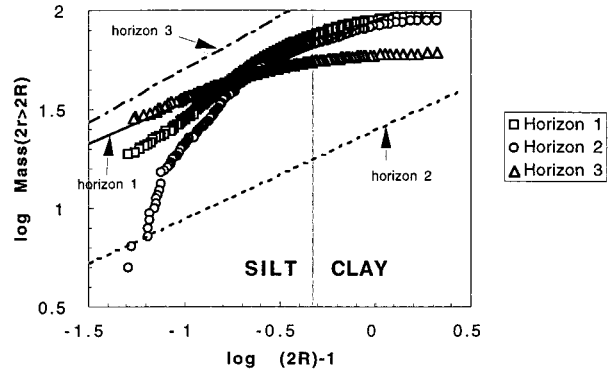


**FIGURE 2. log mass vs log(2*R*)$^{-1}$ for only the silt and clay fractions for the 3 horizons. Lines are the regressions lines shown on Figure 1.**

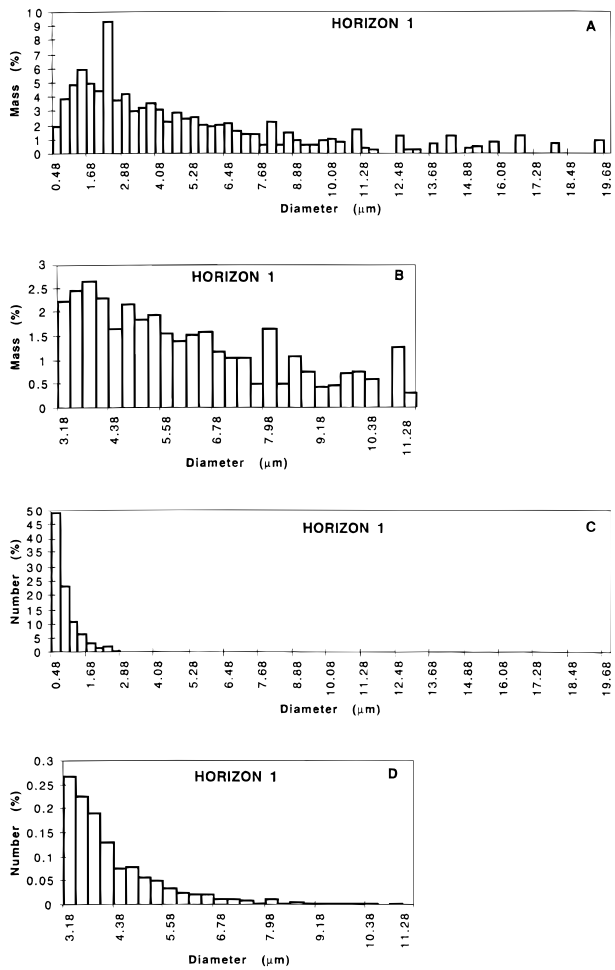


**FIGURE 3. Mass distribution (expressed in percent) of the particles of the horizon 1: (A) from 0.48 to 20 $\mu$m and (B) from 3.18 to 11.28 $\mu$m. Number distribution (expressed in percent) of the particles of the horizon 1: (C) from 0.48 to 20 $\mu$m and (D) from 3.18 to 11.28 $\mu$m.**

## Results and Discussion

**Characteristics of Soil: Description and Soil Size Distribution.** The association Lake Charles–urban complex is described by the National Cooperative Soil Survey (*33*) as "somewhat poorly drained, very slowly permeate, clayed and loamy soils." This association belongs to the typical Uderts Vertisols developed along the Texas gulf coast from fluviatil sediments (*34*). Characteristics of the three soil horizons sampled in this study are summarized in Table 1. The average organic carbon content (OC) is low (<1%) and smectites are

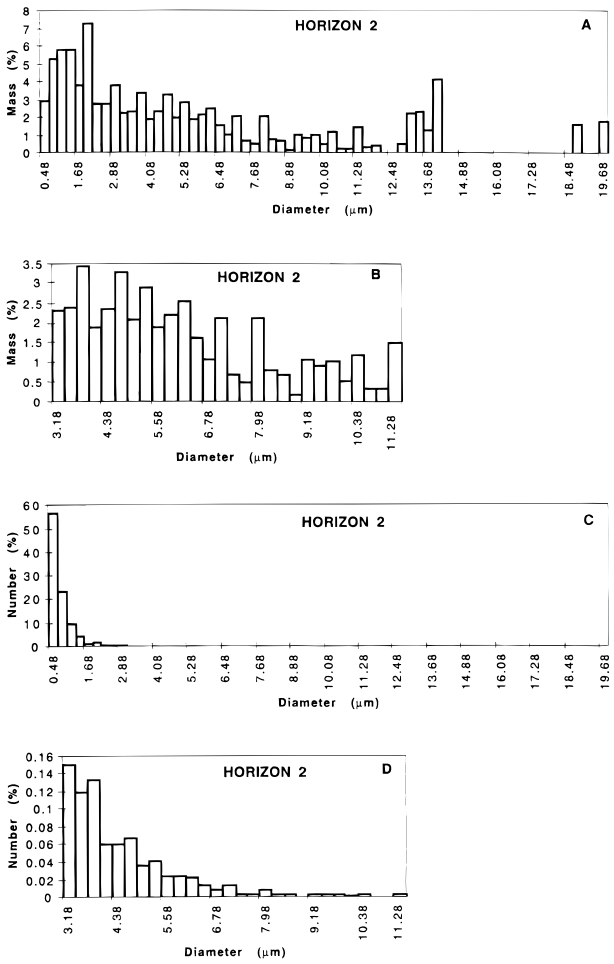


**FIGURE 4. Mass distribution (expressed in percent) of the particles of the horizon 2: (A) from 0.48 to 20 $\mu$m and (B) from 3.18 to 11.28 $\mu$m. Number distribution (expressed in percent) of the particles of the horizon 2: (C) from 0.48 to 20 $\mu$m and (D) from 3.18 to 11.28 $\mu$m.**

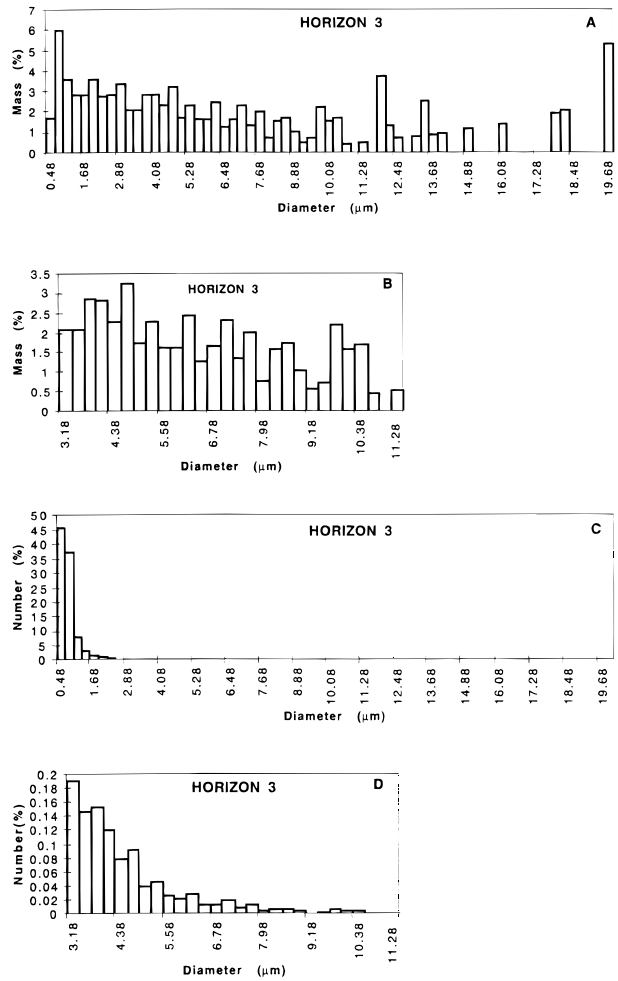


**FIGURE 5. Mass distribution (expressed in percent) of the particles of the horizon 3: (A) from 0.48 to 20 $\mu$m and (B) from 3.18 to 11.28 $\mu$m. Number distribution (expressed in percent) of the particles of the horizon 3: (C) from 0.48 to 20 $\mu$m and (D) from 3.18 to 11.28 $\mu$m.**

the main clay minerals. The three horizons are visually quite distinct. The top horizon is contained within approximately the upper 50 cm and is composed of a very firm dark gray clay. The middle horizon (approximately 30 cm thick) is a very firm, yellowish red clay, while the deepest layer (about 30 cm thick) is a very firm, yellowish brown clay with light olive brown concretions. A similar pH was measured for the three horizons with a value around 8.20. One concludes that the silt fraction is dominant in the first and second horizons (>50%) independent of the size characterization technique used (sieves and sedimentation or particle counter). In the third horizon, the percentages of silt and clay (33.43 and 38.57, respectively) are similar (Table 2). The particle counter provides very detailed information on the clay fraction; however, it is not able to detect particles with diameters less than approximately 0.48 $\mu$m. Comparing the total mass analyzed by the particle counter to the mass actually added to the initial solution and recognizing that the assumed density for conversion from volume to mass likely represents a maximum, we estimate that 6.79, 10.47, and 33.39% of the "clay" mass is composed of particles smaller than 0.48 $\mu$m for horizons 1, 2, and 3, respectively. These particles belong to the colloidal fraction and are typically included in the clay fraction by the soil scientists. The three horizons analyzed correspond in the USDA classification as loam soil, silty-clay soil, and clay-loam soil for, respectively, horizons 1, 2, and 3 (Table 2).

**Power-Law Fits.** A plot of the log of particle mass (mass) vs the log of inverse particle diameter ($2R^{-1}$) is shown in Figure 1 for the three horizons. Only data for the sand and gravel fractions obtained by sieving were used to obtain the regression lines and calculate the slope and fractal dimension (D) for each horizon (Table 3). All the horizons have values of $D$ close to 3, similar to the results reported by Tyler and Wheatcraft (*35*) for clay and silty soils. The goodness of fit ($R^2$) and standard errors (se) of parameter estimates (Table 3) confirm the hypothesis of a linear relationship between the variables plotted (Figure 1). If the scale is changed to the clay and silt fractions, the scaling property should continue and the regression lines should be the same. However, when only these finer fractions are plotted (Figure 2), it is obvious that the regression lines obtained before do not fit over the entire range of particle diameters. In horizons 1 and 2, the silt fraction accounts for the highest percentage of mass with no more than 32% of the mass attributable to the other fractions, and in the horizon 3, clay and silt quantities are quite similar (Table 2). If a regression line is fit for different size intervals (Figure 2) for each horizon, the values obtained for the slope vary from 0 to 3, corresponding to fractal dimensions ($D$) of 3 to 0. In other words, we can obtain all the possible values for $D$ by selecting different ranges of particle size. This means that depending on the scale selected to calculate $D$, the same horizon will yield different fractal dimensions. Moreover, in some cases, this value can even be negative. This has been reported previously by Logsdon et al. (*23*). Similar observations have been made by

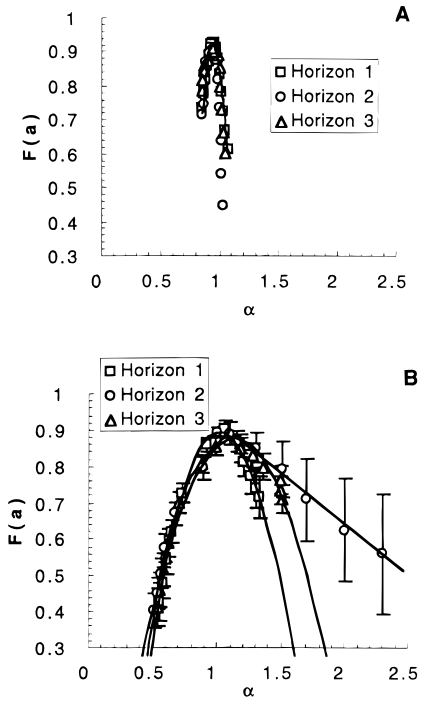


**FIGURE 6. Multifractal spectrum expressed by F(α) vs α plot for the horizons 1, 2, and 3: (A) using the mass distribution as measure and (B) using the number distribution as measure.**

investigators attempting to fit PSD data on particle suspensions from aquatic environments to a power law and estimate values for the power-law exponent $\beta$ (see, for example, ref *36*).

**Self-Similar Measure.** We propose that because the PSD is a measure rather than a geometric object, that the measure itself may display self-similarity. If this is the case, it should be possible to describe the data as a multifractal and a plot of $f[\alpha(q)]$ as function of $\alpha(q)$ should yield a single-humped curve. The point at which a line with slope of unity is tangent with this curve yields the entropy dimension.

Inspection of the mass (Figures 3a, 4a, and 5a) and number distributions (Figures 3c, 4c, and 5c) reveals that the distribution from 0.48 to 20 $\mu$m of particle diameter has a similar profile to the same distribution plotted from 3.18 to 11.28 $\mu$m (Figures 3b, 4b, and 5b for the mass distribution and Figures 3d, 4d, and 5d for the number distribution). This is particularly evident in the number distributions. That is, the shape of the PSD is similar at different scales of resolution. The high resolution of the PSD (more than 150 data points) produced by ESZ-based particle counters provides sufficient data to perform a multifractal analysis of the measures (both mass and number).

The multifractal spectrum for both measures (mass distribution in Figure 6a and number distribution in Figure 6b) calculated for the three horizons using eqs 12 and 13 as described in the Materials and Methods exhibit multifractal behavior characterized by a convex curve (*20*). The mass distributions for the three horizons result in similar spectra (Figure 6a) with a common amplitude in $\alpha$ ($\alpha_{min} = 0.4$ and $\alpha_{max} = 1.1$). In contrast, the spectra calculated from the number distributions (Figure 6b) are more spread out with a common $\alpha_{min} = 0.5$ and different $\alpha_{max}$ depending on the horizons (1.7, 2.4, and 2.5 for, respectively, horizons 1, 2, and 3). In this case, the greatest differences between spectra for the number distributions are observed for the negatives values of $q$. This means that these distributions differ most in the smallest values of the measure (number %) while the largest values of the measure are quite similar. Comparing the spectra obtained from the two measures, a significant difference in the amplitude of the Lipschitz–Hölder exponent, $\alpha$, is observed. When the $\alpha$ amplitude is bigger, singularities of the measures are more pronounced and the self-similarity behavior is clearer.

**TABLE 4. Entropy Dimension of the Three Horizons for Both Measures, Number and Mass Distributions**

| | particle number distribution | | mass distribution | |
|---|---|---|---|---|
| horizon | α(1) | se | α(1) | se |
| 1 | 0.727 | 0.027 | 0.924 | 0.007 |
| 2 | 0.672 | 0.031 | 0.863 | 0.023 |
| 3 | 0.702 | 0.029 | 0.857 | 0.026 |

As discussed previously, the entropy dimension, $\alpha(1)$, is an important parameter of the spectrum. In the cases considered here, possible values of the entropy dimension are $0 < \alpha(1) < 1$. A value of 1 signifies an evenly spread distribution of irregularities across the particle sizes. When $\alpha(1) < 1$, there is a subset of particle sizes (the domain of the measure) in which the irregularities concentrate. The entropy dimensions [$\alpha(1)$] for the three horizons obtained from the mass distribution are larger than 0.85 [$\alpha(1) < 1$] (Table 4). Therefore, the values of $\alpha(1)$ found in these three horizons reflects a degree of "emptiness" of the irregularities present in the data set that is quite similar. It is also significant that the values of $\alpha(1)$ obtained from the particle number distribution for the three horizons are lower than those obtained from the mass distribution. This indicates that the distribution in particles number is more concentrated than that for mass as previously shown in Figures 3, 4, and 5. The entropy dimension may be a useful statistic for comparing properties of soils, sediments, and suspensions. We conclude that simple power laws are not likely to be applicable to PSD data from many natural systems as a general case. Rather, these data may be more appropriately described as multifractal.

## Acknowledgments

We thank M.A. Martin, F.J. Caniego and F.J. Taguas for their helpful discussion of multifractal concepts and S. Veerapaneni for his useful explanations in using the particle counter. This work was supported in part by funding from U.S. Environmental protection Agency Hazardous Substance Research Center, South/Southwest and the National Science Foundation.

## Literature Cited

(1) Amal, R.; Raper, J. A.; et al. *J. Colloid Interface Sci.* **1990**, *140* (1), 158–168.
(2) Jiang, Q.; Logan, B. E. *Environ. Sci. Technol.* **1991**, *25* (12), 2031–2038.
(3) Logan, B. E.; Wilkinson, D. B. *Biotechnol. Bioeng.* **1991**, *38*, 389–396.
(4) Da-Hong, L.; Ganczarczyk, J. *Environ. Sci. Technol.* **1989**, *23* (11), 1385–1389.
(5) Wiesner, M. R.; Mazounie, P. *J. Am. Water Works Assoc.* **1989**, *81*, 80–89.
(6) Wu, M. K.; Friedlander, S. K. *J. Colloid Interface Sci.* **1993**, *159*, 246–248.
(7) Hartmann, W. K. *Icarus* **1969**, *10*, 201–213.
(8) Turcotte, D. L. *J. Geophys. Res.* **1986**, *91*, 1921–1026.
(9) Turcotte, D. L. *Pure Applied Geophys.* **1989**, *131*, 171–196.
(10) Thompson, A. H.; Kartz, A. J.; Krohm, C. E. *Adv. Phys.* **1987**, *36*, 625–694.
(11) Tyler, S. W.; Wheatcraft, S. W. *Soil Sci. Soc. Am. J.* **1989**, *53*, 987–996.
(12) Tyler, S. W.; Wheatcraft S. W. *Water Resour. Res.* **1990**, *26*, 1047–1054.
(13) Clapp, R. B.; Hornberger, G. M. *Water Resourc. Res.* **1978**, *14*, 601–604.

(14) Hillel, D. *Fundamentals of soil physics*; Academic Press: New York, 1980.
(15) Bartoli, F.; Philippy, R.; Burtin, G. *J. Soil Sci.* **1988**, *39*, 593−616.
(16) Bartoli, F.; Philippy, R.; Doirisse, S.; Niquet, S.; Dubuit, M. *J. Soil Sci.* **1991**, *42*, 167−185.
(17) Bui, E. N.; Mermut, A. R.; Santos, M. C. D. *Soil Sci. Soc. Am. J.* **1989**, *53*, 661−665.
(18) Mandelbrot, B. B. *The fractal geometry of nature*; Freeman W. H.; New York, 1983.
(19) Burrough, P. A. *J. Soil Sci.* **1983**, *34*, 577−597.
(20) Feder, H. *Fractals*; Plenum Press: New York, 1988.
(21) Falconer, K. *Fractal geometry*; John Wiley & Sons: Chichester, England, 1990.
(22) Wu, Q.; Borkovec, M.; Sticher, H. *Soil Sci. Soc. Am. J.* **1993**, *57*, 883−890.
(23) Logsdon, S. D.; Gimenez, D.; Allmaras, R. R. *Soil Sci. Soc. Am. J.* **1996**, *60*, 1327−1330.
(24) Perfect, E.; Kay, B. D.; Rasiah, V. *Soil Sci. Soc. Am. J.* **1993**, *57*, 896−900.
(25) Sreenivasan, K. R. *Annu. Rev. Fluid Mech.* **1991**, *23*, 539−600.
(26) Evertsz, C. J. G.; Mandelbrot, B. B. In *Chaos and Fractals: New Frontiers of Science*; Peitgen, H., Jurgens, H., Saupe, D., Eds.; Springer-Verlag: New York, 1992; pp 921−953.
(27) Folorunso, O. A.; Puente, C. E.;. Rolston, D. E.; Pinzon, J. E. *Soil Sci. Soc. Am. J.* **1994**, *58*, 284−294.
(28) Hendershot, W. H.; Lalande, H.; Duquette, M. In *Soil sampling and methods of analysis*; Carter, M. R., Ed.; Canadian Society of Soil Science, 1993, pp 141−145.
(29) Head, K. H. In *Manual of soil laboratory testing*, 2nd ed.; Pentech Press: London, 1992; Vol. I.
(30) Coulter Electronics Limited: *Fine Particle Application notes for Coulter Counters*; Coulter Electronics Limited: England, 1987.
(31) Culley, J. L. B. In *Soil sampling and methods of analysis*; Carter M. R., Ed.; Canadian Society of Soil Science, 1993, pp 529−539.
(32) Chhabra, A.; Jensen, R. V. *Phys. Rev. Lett.* **1989**, *62*, 1327−1330.
(33) Wheeler, F. F. *Soil Survey of Harris County, Texas*; USDA, 1976.
(34) Fofth, H. D.; Schafer, J. W. *Soil geography and Land use*; John Wiley & Sons: 1980.
(35) Tyler, S. W.; Wheatcraft, S. W. *Soil Sci. Soc. Am. J.* **1992**, *56*, 362−369.
(36) O'Melia, C. R. *Coagulation in Wastewater treatment: The Scientific Basis of Flocculation*; Sijthoff and Noordhoff: The Netherlands, 1978.

*Received for review May 20, 1997. Revised manuscript received February 3, 1998. Accepted February 4, 1998.*

ES9704343